Astron. Astrophys. 134, 185–188 (1984)

ASTRONOMY AND ASTROPHYSICS

Research Note

An example of a solar S-component model calculation using force-free magnetic field extrapolation

J. Hildebrandt[1], **N. Seehafer**[1], **and A. Krüger**[2]

[1] Zentralinstitut für solar-terrestrische Physik (HHI) der Akademie der Wissenschaften der DDR, Sonnenobservatorium Einsteinturm, DDR-1500 Potsdam, Telegrafenberg, German Democratic Republic
[2] Zentralinstitut für solar-terrestrische Physik (HHI) der Akademie der Wissenschaften der DDR, DDR-1199 Berlin, Rudower Chaussee 5, German Democratic Republic

Received May 16, accepted December 13, 1983

Summary. As a first example of extensive model calculations we present radio emission features calculated for the solar active region McMath 12417 on July 4, 1973 using force-free extrapolated magnetic fields with constant α. The magnetic field data were derived from magnetographic measurements, and height distributions of temperature and electron density from a semi-empirical sunspot model by Staude (1981) based on recent X–, EUV–, and optical data. In contrast to the rather simple magnetic field structure, a complex structure of the S-component source at a test wavelength of 6 cm is obtained, exhibiting a dip of brightness temperature above the sunspot centre, a weakly polarized pseudo-loop structure at maximum intensity surrounding the centre, and a ring of high circular polarization at the outer edge of the source.

Key words: solar radio emission – radiative transfer – magnetic fields

Observations of solar active regions with high spatial resolution in the microwave range have stimulated some progress in the field of emission models of the S-component (cf. e.g. Gelfreikh and Lubyshev, 1979; Alissandrakis et al., 1980; Pallavicini et al., 1981; Krüger et al., 1983). By means of the emission models the role of the contributions of Coulomb bremsstrahlung and gyromagnetic radiation and other features can be checked for different spatially distributed parts of source regions of the S-component emission. But as a matter of fact all computations of emission quantities critically depend on the applied distributions of the input plasma parameters, viz. temperature T, electron density N_e, and magnetic field $\boldsymbol{B}$. While principally based on the same main concepts of radiation processes the existing variety of S-component models concerns just the use of quantitatively different parameter distributions. A special role is here played by the magnetic field because all positions of the gyroresonance layers and their consequence on the opacity of gyromagnetic radiation as well as the polarization effects of (optically thin) bremsstrahlung etc. sensitively depend on the magnetic vector.

In recent time, therefore, some approaches were undertaken to use magnetic field models based on real photospheric observations and theoretical extrapolations of these fields to greater heights of the solar atmosphere, e.g. by Alissandrakis (1980), Pallavicini et al. (1981), and Schmahl et al. (1982).

However, the considerable effort in treating the radiative transfer for a sufficiently large number of ray trajectories led these authors to introduce more or less stringent simplifications to the model of the thermodynamic parameters (N_e, T) or the geometry of the magnetic field. The present communication reports briefly about results of model calculations combining both advanced model distributions of the thermodynamic plasma parameters and a three-dimensional nonsymmetric magnetic field distribution derived from real observations, extrapolated under the assumption of a force-free field with constant α (α defined by the equation $\nabla \times \boldsymbol{B} = \alpha \boldsymbol{B}$).

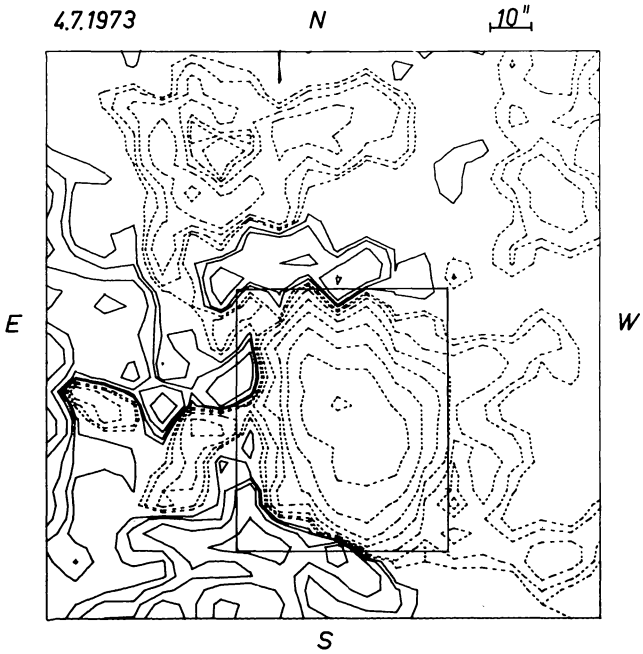

Fig. 1a. Photoelectric magnetogram ($B_{\|}$) obtained at the Solar Observatory Einsteinturm in Potsdam on July 4, 1973, 08.30 UT. Contour levels are 20, 40, 80, 160, 320, 640, 1280, and 2560 G. Solid lines refer to positive, dashed to negative fields. The inner rectangular part denotes the region applied for the radio model calculations (cf. Fig. 2)

Send offprint requests to: J. Hildebrandt

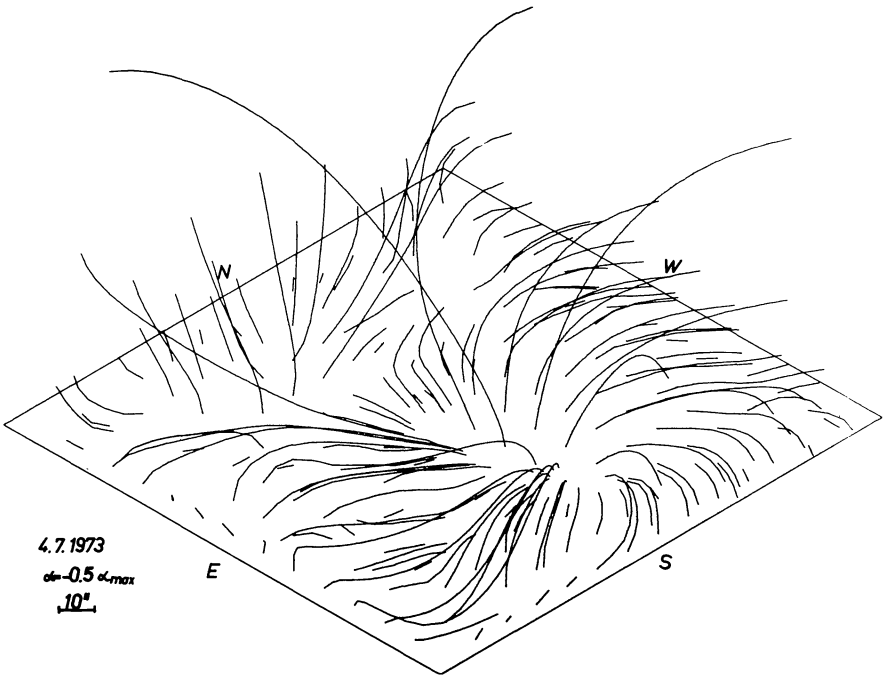

Fig. 1b. Perspective view of the lines of force above the area of Fig. 1a extrapolated under the assumption $\alpha = -0.5\alpha_{max}$ (the optimum value by comparison with Hα photographs)

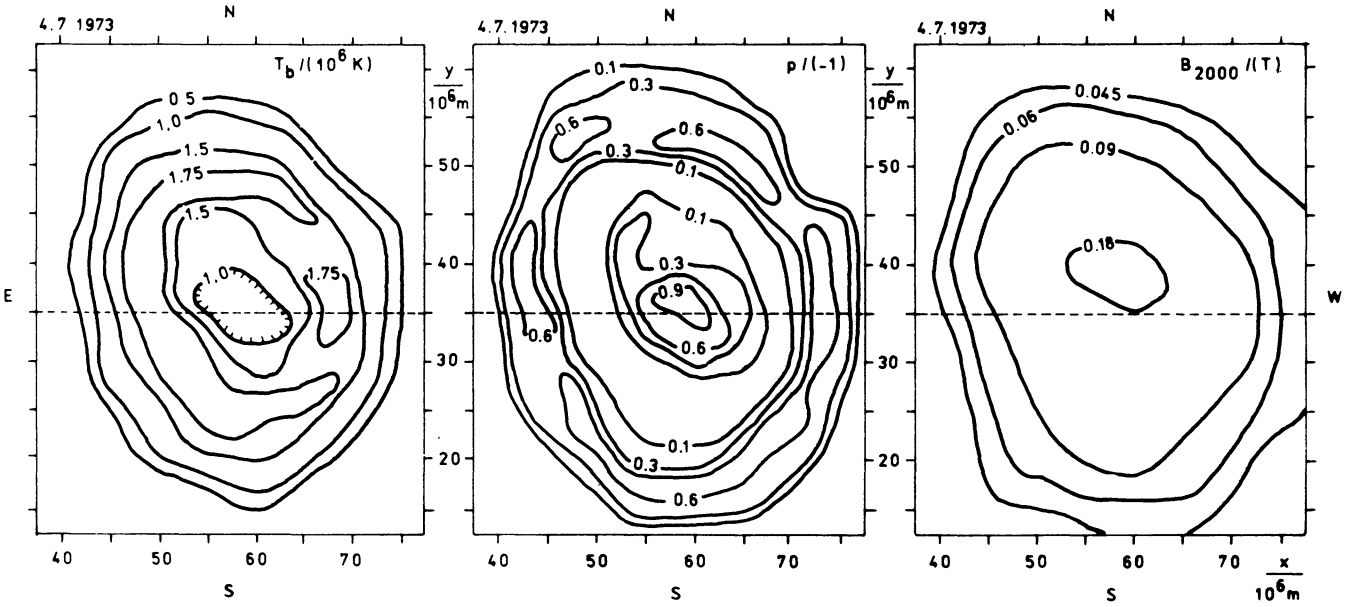

Fig. 2a–c. Results of model calculations for 4.9 GHz: **a** Isolines of brightness temperature. **b** Representation of the degree of circular polarization. **c** Isolines of the magnetic field at the bottom of the corona (2000 km above the photosphere) corresponding to the first four harmonics of the gyrofrequency

The S-component emission model used here was described by Hildebrandt (1983) and Krüger et al. (1983). For the purpose of application to a real active region we selected the simple spot group of July 4, 1973 for which reliable and well studied magnetic field observations of the Solar Observatory Einsteinturm at Potsdam were available (cf. Seehafer and Staude, 1980). The position of the region selected was close to the disk center, hence effects of polarization varying outside the source region can be disregarded. The magnetogram used had a horizontal extension of about 100,000 km × 100,000 km with a spatial resolution of approximately 5000 km. The method of extrapolation applied was that of Seehafer (1978, 1979); a comparison of different methods of extrapolation, applied to the region considered here, was published by Seehafer (1982). The magnetogram and a field line picture of the active region investigated are shown in Fig. 1.

The results of our calculations (which were restricted to the part of strongest magnetic field with an extension of 40,000 km × 50,000 km, cf. Fig. 1a) are presented in Fig. 2. Figure 2a shows the brightness temperature distribution computed at a wavelength of 6 cm (4.9 GHz) over the source region. In contrast to the magnetic field distribution derived, which is shown in Fig. 2c for a height level of 2000 km above the photosphere, the distribution of the radio emission is more complex due to the dependence of the gyromagnetic emission on the angle θ between the ray path and the magnetic field vector which changes from point to point. An even more complex picture is obtained for the distribution of the degree

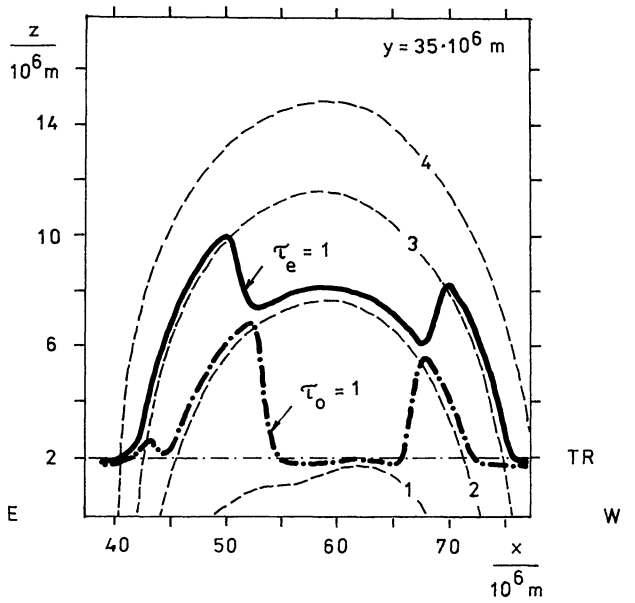

Fig. 3a. Vertical cross section through the emission volume at $y=35{,}000$ km showing gyroresonance levels for 4.9 GHz (thin dashed lines) and levels where $\tau_{o,e}=1$ (heavy lines). TR – transition region to the corona

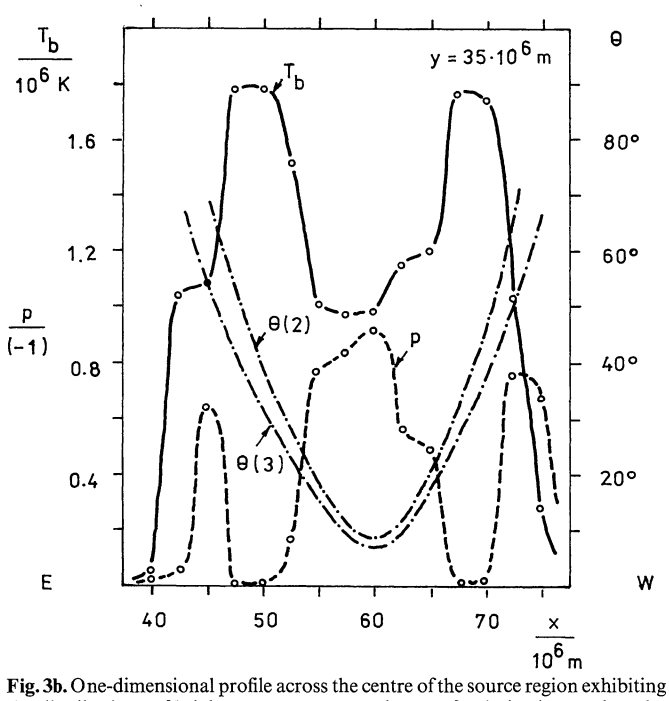

Fig. 3b. One-dimensional profile across the centre of the source region exhibiting the distributions of brightness temperature, degree of polarization, and angles between $\boldsymbol{B}$ and z for $s=2, 3$

of (extraordinary) circular polarization (Fig. 2b) which presents a highly structured pattern. This pattern is mainly due to the influence of different harmonics of the gyrofrequency in different points of the region. The outer edge of the polarized emission is due to the influence of the third harmonic; higher harmonics than the third are not detectable for active regions near the centre of the solar disk, as is well known. A special feature differing from the ideal magnetic dipole model is the occurrence of polarized islands in the outer ring of polarized emission.

A cross-section through the central part of the radio emission volume is presented in Fig. 3a. In addition to the levels $\nu=sv_B$ (thin dashed lines), the height at which the total optical depths become greater than unity is marked by heavy lines for both the extraordinary (solid line) and ordinary mode (chain line), respectively. For comparison, in Fig. 3b the characteristics calculated are shown in a profile through the source centre (dashed line in Fig. 2). From this figure the different distributions of the three parameters: brightness temperature T_b, degree of (circular) polarization p, and angle θ between the magnetic field vector and the line of sight at the height of the second [$\theta(2)$] and third [$\theta(3)$] harmonic level are clearly demonstrated. The centre of the emission region is characterized by a maximum of the degree of polarization, a minimum of $\theta(s)$, and also by a dip of the brightness temperature (which is due to the vanishing ordinary mode emission for small angles θ). The maximum of brightness corresponds to a minimum of polarization and at the outer flanks of the brightness distribution, a ring of strong polarization appears.

The figures discussed illustrate the fact that even with relatively simple magnetic field configurations, and uniformly distributed thermodynamic parameters, a rather complex radio emission pattern results. In particular the relative minimum of brightness in the source centre has nothing to do with a decrease of electron temperature there. Also, the loop-like horse-shoe structure in Fig. 2a cannot be related to any actual loop structure of the source region but is a mere consequence of the asymmetry of the magnetic field.

Our results are similar to those of Alissandrakis et al. (1980), but somewhat different from those of Gelfreikh and Lubyshev (1979), especially with regard to the maximum of p and the relative minimum of T_b in the innermost part of the spot. Further differences concern the detailed positions and widths of the rings. Unfortunately the paper of Gelfreikh and Lubyshev does not contain information about the scale and the magnitude of the magnetic field on which these positions depend.

Recently observations of horse-shoe structures were reported by Lang et al. (1982). Some source structures calculated are quite similar to those observed by Alissandrakis and Kundu (1982) on May 27, 1980 with WRST. A detailed study of that extended region, by means of an extrapolated field analysis, is now in progress.

Although the resulting radiation pattern of S-component gyromagnetic emission is governed by the magnetic field, the term "coronal magnetogram" (Kundu et al., 1977) sometimes used for radio maps of solar active regions should not be misinterpreted, because in contrast to optical (photospheric) magnetograms, radio observations in general do not refer to a fixed height level in the solar atmosphere (cf. Fig. 3a) and cannot be directly interpreted in terms of iso-gauss profiles unless three-dimensional model analyses are carried out.

Acknowledgements. The authors would like to thank Dr. J. Staude for stimulating discussions. They are also indebted to Dr. K. Pflug for a critical reading of the manuscript.

References

Alissandrakis, C.E.: 1980, in *Radiophysics of the Sun*, eds. M. R. Kundu, T. Gergely, Reidel, Dordrecht, p. 101
Alissandrakis, C.E., Kundu, M.R.: 1982, *Astrophys. J.* **253**, L49

Alissandrakis, C.E., Kundu, M.R., Lantos, P.: 1980, *Astron. Astrophys.* **82**, 30
Gelfreikh, G.B., Lubyshev, B.I.: 1979, *Astron. Zhurn.* **56**, 562
Hildebrandt, J.: 1983, Doctoral Thesis, Akademie der Wissenschaften, Berlin
Krüger, A., Hildebrandt, J., Fürstenberg, F., Staude, J.: 1983, HHI-STP-Report Nr. 14, Berlin
Kundu, M.R., Alissandrakis, C.E., Bregman, J.D., Hin, A.C.: 1977, *Astrophys. J.* **213**, 278
Lang, K.R., Willson, R.F.: 1982, *Astrophys. J.* **255**, L111
Pallavicini, R., Sakurai, T., Vaiana, G.S.: 1981, *Astron. Astrophys.* **98**, 316
Schmahl, E.J., Kundu, M.R., Strong, K.T., Bentley, R.D., Smith, J.B., Jr., Krall, K.R.: 1982, *Solar Phys.* **80**, 233
Seehafer, N.: 1978, *Solar Phys.* **58**, 215
Seehafer, N.: 1979, Doctoral Thesis, Akademie der Wissenschaften, Berlin
Seehafer, N.: 1982, *Solar Phys.* **81**, 69
Seehafer, N., Staude, J.: 1980, *Solar Phys.* **67**, 121
Staude, J.: 1981, *Astron. Astrophys.* **100**, 284